Published in final edited form as:
Biomacromolecules. 2008 July ; 9(7): 1818–1825. doi:10.1021/bm800031t.

Polyphosphazene/Nano-Hydroxyapatite Composite Microsphere Scaffolds for Bone Tissue Engineering

Syam P. Nukavarapu[1], **Sangamesh G. Kumbar**[1], **Justin L. Brown**[2], **Nicholas R. Krogman**[3], **Arlin L. Weikel**[3], **Mark D. Hindenlang**[3], **Lakshmi S. Nair**[1], **Harry R Allcock**[3], and **Cato T. Laurencin**[1,2,4,*]

[1]Department of Orthopaedic Surgery, University of Virginia, Virginia 22908

[2]Department of Biomedical Engineering, University of Virginia, Virginia 22908

[3]Department of Chemistry, The Pennsylvania State University, Pennsylvania 16802

[4]Department of Chemical Engineering, University of Virginia, Virginia 22904

Abstract

The non-toxic, neutral degradation products of amino acid ester polyphosphazenes make them ideal candidates for *in vivo* orthopaedic applications. The quest for new osteocompatible materials for load bearing tissue engineering applications has led us to investigate mechanically competent amino acid ester substituted polyphosphazenes. In this study, we have synthesized three biodegradable polyphosphazenes substituted with side groups namely leucine, valine and phenylalanine ethyl esters. Of these polymers, the phenylalanine ethyl ester substituted polyphosphazene showed the highest glass transition temperature (41.6 °C) and hence was chosen as a candidate material for forming composite microspheres with 100 nm sized hydroxyapatite (nHAp). The fabricated composite microspheres were sintered into a three-dimensional (3-D) porous scaffold by adopting a dynamic solvent sintering approach. The composite microsphere scaffolds showed compressive moduli of 46–81 MPa with mean pore diameters in the range of 86–145 μm. The three-dimensional polyphosphazene-nHAp composite microsphere scaffolds showed good osteoblast cell adhesion, proliferation and alkaline phosphatase expression, and are potential suitors for bone tissue engineering applications.

Keywords

biodegradable; polyphosphazene; nano-hydroxyapatite; composites; microspheres; 3-D-scaffolds; osteoblasts; adhesion; proliferation; bone tissue engineering

1. Introduction

Polyphosphazenes are a unique class of polymers with synthetic flexibility and a high degree of freedom in modulating physical and chemical properties. They are organic-inorganic hybrid polymers with alternating phosphorus and nitrogen atoms in the backbone with every phosphorous atom bearing two organic side groups as shown in Figure 1a.[1] To date, researchers have derived a large number of polymers, using poly(dichlorophosphazene) as a reaction platform, with great diversity in the polymer properties for applications ranging from stable

*Corresponding Author, Cato T. Laurencin M.D., Ph.D., University Professor, Lillian T. Pratt Distinguished Professor and Chair of Orthopaedic Surgery, Professor of Biomedical and Chemical Engineering, The University of Virginia, 400 Ray C. Hunt Drive, Suite 330, Charlottesville, VA 22903, Office: (434) 243-0250, Fax: (434) 243-0252, Email: laurencin@virginia.edu.

biocompatible materials to controlled degrading materials for tissue engineering and drug delivery applications.[2] Biodegradable polyphosphazenes with hydrolytically sensitive organic side groups such as amino acid esters, glucosyl, glyceryl, and lactide and glycolide esters have raised interest as biomaterials.[2] Among these polymers, amino acid ester derivatives have attracted much attention for biomedical applications because of the fine control of hydrolytic degradation coupled with neutral non-toxic by-products.[2,3] Unlike PLAGA, the degradation products of many polyphosphazenes form a buffering system (ammonium phosphate) that maintains neutral pH throughout the degradation.[1,4] Hydrolysis times and the rates depend on the side groups linked to the polymer backbone. The choice of hydrolytically labile groups results in faster degradation, and such systems find applications in drug delivery. A combination of both hydrophilic and hydrophobic side groups results in prolonged degradation that suggests applications as controlled degradable materials for tissue engineering applications.[5] Along with the poly(anhydride)s and poly(ortho ester)s, polyphosphazenes also can be tuned to achieve surface degradation, bulk degradation or mixed degradation based on the application requirement.[5,6]

A series of polyphosphazenes in the form of two dimensional films showed good osteoblast cell adhesion and proliferation. [7,8] We have further demonstrated the tissue compatibility and the *in vivo* degradation of alanine ethyl ester based polyphosphazenes in a rat model.[9] The *in vitro* and *in vivo* observations confirmed the osteocompatibility nature of polyphosphazenes and hence these materials are good candidates for bone tissue engineering applications.

Scaffold based tissue engineering has become a promising strategy in regenerative medicine, because cells alone lack the ability to form three dimensional tissues without the support of an artificial structure, often referred to as a scaffold. Various synthetic and natural polymers have already been adopted for 3-D scaffold fabrication. Techniques such as solvent casting and particulate leaching, gas foaming, freeze drying, electrospinning, and phase separation have been used traditionally for 3-D scaffold fabrication. Microsphere sintering technology is yet another promising method developed for bone tissue engineering applications.[10,11] In previous studies, PLAGA sintered 3-D microsphere scaffolds with 25–30% pore volume and ~150 μm median pore size performed well for bone tissue regeneration.[10]

The aim of the present study was to develop, and characterize polyphosphazene-nano-hydroxyapatite (nHAp) composite microsphere scaffolds for bone repair and regeneration. In this study, three different single-substituent polyphosphazenes (with side groups: leucine, valine and phenylalanine ethyl esters) were synthesized in an attempt to achieve a polymer with a glass transition temperature higher than physiological temperature in order to maintain structural integrity in an *in vivo* environment. It is hypothesized that bulk amino acid side groups involved in this study yield polymers with high T_g values suitable for load bearing tissue engineering applications. One of the high glass transition polymers, poly[*bis*(ethyl phenylalanato)phosphazene] (PNEPhA), was combined with 20 wt% nHAp and fabricated into 3-D microsphere scaffolds using a novel dynamic solvent sintering method. We further determined the usefulness of these scaffolds for bone tissue engineering by subjecting them to mechanical and porosity evaluation. In addition, this paper describes the *in vitro* osteocompatibility of polyphosphazene-nHAp composite scaffolds by culturing primary rat osteoblast cells, and comparing them to the PLAGA-nHAp composite scaffolds.

2. Materials and Methods

2.1. Materials

Poly(D-L-85 lactide-*co*-15 glycolide) (PLAGA) of inherent viscosity 0.60 – 0.80 dL/g was purchased from Lakeshore Biomaterials (Birmingham, AL). Hydroxyapatite dry powder with an average particle size of 100 nm (specific surface area: 50–70 m^2/g) was obtained from

Berkeley Advanced Biomaterials, Inc., Berkeley, CA. Methylene chloride, *n*-heptane, *n*-hexane, tetrahydrofuran (THF) and ascorbic acid were procured from Fischer Scientific (Hampton, NH). Poly(vinyl alcohol) (PVA), β-glycerophosphate and the anhydrous solvents THF, triethylamine (TEA) and toluene for polyphosphazene synthesis were obtained from EMD (Darmstadt, Germany). Leucine, valine, and phenylalanine ethyl ester hydrochloride side groups were also obtained from Bachem (Torrance, California). Ham's F-12 nutrient mixture, fetal bovine serum (FBS), penicillin/streptomycin (PS) and phosphate buffer saline (PBS, 1X) were procured from Invitrogen Corporation (Carlsbad, CA).

2.2. Polymer synthesis

Single-substituent polyphosphazene with the amino acid ethyl ester side groups of leucine, valine, and phenylalanine were synthesized with similar techniques.[3,7] Hexachlorotriphosphazene was purified by recrystallization, followed by sublimation. This was then polymerized under vacuum in a sealed silica tube at 255 °C to obtain poly (dichlorophosphazene) (PDCP), followed by sublimation of unreacted hexachlorocyclotriphosphazene. A representative synthetic protocol for phenyl alaninato ethyl ester is described. The reaction was carried out under dry argon using standard Schlenk line techniques. PDCP (17 g, 0.146 mol) was dissolved in 1.7 L of dry THF. Phenylalanine ethyl ester hydrochloride (202 g, 0.879 mol) was suspended in 1 L of dry THF and 734 mL (5.28 mol) triethyl amine. This suspension was refluxed overnight, then filtered and added drop wise to the polymer solution. Reaction progress was monitored by recording ^{31}P NMR spectra, and was continued (12–48 hours) until complete side group substitution was identified by the presence of a single broad ^{31}P peak at approximately 0 ppm. Subsequently, the reaction mixture was filtered, and precipitated in hexane, followed by precipitation into methanol (three times) to completely remove the triethylamine hydrochloride salt particles. All the polymers under study showed yields around 85%.

2.3. Polymer Characterization

Polymers were dried and characterized for their chemical structure and the side group substitution using ^{31}P NMR (145 MHz) and ^{1}H at 360 MHz (Bruker 360 MHz NMR spectrometer). Both ^{31}P and ^{1}H NMR chemical shifts recorded for the polymers under study match the literature values.[3] Molecular weights of the polymers were measured via gel permeation chromatography (GPC) by use of a Hewlett Packard LC 1100 series. Molecular weights were compared to polystyrene standards. Differential scanning calorimetry (TA instruments, DSC Q1000), with ca. 10 mg per sample, was used to obtain glass transition temperature (T_g) for all the polymers under study. Polymer samples were heated and cooled (−70 to 100 °C, three cycles) at a heating rate of 3 °C/min under a nitrogen atmosphere, and the T_g was determined from the half height point of the heat capacity change in the thermogram.

2.4. Polyphosphazene-nHAp composite microsphere preparation

Poly[*bis*(ethyl phenylalaninato)phosphazene] (Figure 1b), with a weight average molecular weight (M_w) of 130 kD, and nHAp were mixed in 9:1, 8:2, and 7:3 weight ratios (referred now on as 10, 20 and 30 wt % of nHAp) to form composite microspheres using emulsion/solvent evaporation method. Briefly, the PNEPhA and the corresponding nHAp were dissolved in methylene chloride, ~ 30% (wt./vol.), by vortexing for 3 h, and were poured as a fine continuous flow into a 1% (wt./vol.) PVA solution which was constantly stirred at 250 rpm. The stirring was continued for the next 24 h to allow complete methylene chloride evaporation. The resultant PNEPhA-nHAp composite microspheres were washed with distilled deionized (DDI) water to remove any traces of PVA. Furthermore, microspheres were air dried for 2h, and subjected to vacuum drying using a desiccator. Later, the composite microspheres were sieved

to obtain a 350–500 μm size range and preserved in a desiccator until further use. Similarly, PLAGA microspheres with 20 wt% of nHAp were also prepared with a similar procedure.

2.5. Three dimensional scaffold fabrication using solvent/non-solvent sintering

PNEPhA microspheres (350–500 μm size range) with different loadings of nHAp (10, 20 and 30 wt%) were sintered using a novel solvent/non-solvent method.[12] Solvent/non-solvent systems were composed of solvents such as CH_2Cl_2, $CHCl_3$, and C_4H_8O (THF) and the non-solvent C_6H_{14} (*n*-hexane). Solvent/non-solvent mixtures were added to microspheres in 1:1000 volume to weight ratio and vortexed for 10s before placing into a mold of required shape. A plunger, capable of applying 1.5 g weight for unit area (mm^2), was used to achieve close packing of the microspheres without deforming their spherical shape. The mold, along with the scaffolds, was air dried for 30 min and moved to a desiccator for further drying. In contrast, PLAGA-nHAp microspheres were placed in a mold and heat-treated at 95 °C/2h to form scaffolds. Later, all the scaffolds were lyophilized for further use.

2.6. Microsphere scaffolds: morphology, mechanical strength and porosity

Scanning electron microscopy (SEM) was used to characterize the morphology of the individual microspheres and the corresponding scaffolds. Samples were coated with gold/palladium using a Hummer V sputtering system and examined under a JEOL JSM 840 SEM. Uncoated samples were used for elemental analysis with an energy dispersive X-ray analysis (EDXA) detector coupled with the SEM.

Cylindrical scaffolds (n=6) with 2:1 aspect ratio (10 mm length and 5 mm diameter) were used for mechanical characterization. Compressive testing was carried out using an Instron model 5544 with a cross head speed of 5 mm/min maintained until the sample fails. Compressive modulus and the maximum compressive strength of these scaffolds were determined using the Merlin data analysis software.

Mercury intrusion porosimetry was used to determine the porosity of the scaffolds. Micromeritics Autopore III porosimeter (Norcross, GA) was employed to measure the volume of mercury intrusion at specific pressures for the scaffolds (n=3). The scaffold pore volume and the pore size were calculated by substituting this information into Washburn equation. A set of three scaffolds (8 mm diameter and 2 mm thickness) in a 5 mL penetrometer was used for each measurement.

2.7. Primary rat osteoblast (PRO) cell isolation

Primary rat osteoblast (PRO) cells were isolated from calvaria of 2–3 day old neonatal Sprague-Dawley rats procured from Charles River Laboratories, Inc., Wilmington, MA. The isolation procedure was approved by the University of Virginia, Animal Care and Use Committee, following the guidelines established by the National Institutes of Health. Calvaria were scraped gently and irrigated with PBS with 1% PS to wash off any fat cells and fibroblasts. Thin sheets of calvarias were dissected, minced, and incubated for 45 min with collagenase and trypsin digestion solution. Out of the four consecutive digestions, the first one was discarded for minimizing fibroblast population. The supernatant from the other three digestions were collected and centrifuged along with culture media at 1300 rpm for 7 minutes. The culture media consist of Ham's F-12 media supplemented with 12 % FBS and 1 % PS. The obtained cell pellet was suspended in fresh media and plated in a T 25 flask. Passage number 3 cells were used for cell seeding.

2.8. PRO culture on Polyphosphazene-nHAp microsphere scaffolds

For *in vitro* studies, microsphere scaffolds (8 mm diameter and 2 mm thickness) were sterilized by immersing in 70% ethanol for 30 min. They were then washed thrice in sterile water before exposing to UV radiation (30 minutes on each side inside the cell hood). Scaffolds were placed in 24 well plates and seeded with 50,000 PRO cells on each scaffold. Cell seeded scaffolds were incubated for 2 h to promote the cell attachment before adding 1mL of media to completely submerge the scaffold. Ham's F-12 media (supplemented with 12% FBS, 1% PS, 3mM of β-glycerophosphate, and 10μg/mL of ascorbic acid) was used throughout the study with media replenishing every two days. The culture was maintained for 3, 7, 14, and 21 days in an incubator at 37 °C, 5% CO_2 and 95% humidified air.

2.9. Cell morphology

At predetermined time points of 7, 14 and 21 days, the cell seeded scaffolds (n=2) were taken out of the culture and gently washed with PBS. Cells on scaffolds were fixed with 1 % glutaraldehyde for 1 h and 3 % glutaraldehyde for 24 h at 4 °C. These scaffolds were subjected to sequential dehydration for 10 min each with ethanol series (30%, 50%, 70%, 90% and 100%). Further, scaffolds were allowed to dry for a day and visualized under SEM for cell adhesion and proliferation.

2.10. Immunofluorescence staining for actin and nuclei

Cellularized scaffolds were stained for cytoskeletal actin and cell nuclei and then visualized using a Zeiss LSM 510-UV confocal laser scanning microscope (CLSM, Carl Zeiss MicroImaging, Inc., Thornwood, NY). Briefly, the scaffolds from culture were washed thrice with PBS and fixed with 4% formaldehyde for 20 min. The scaffolds were permeabilized with 0.1% Triton-100 for 5 min, and blocked with 1% BSA solution for 30 min. All the above solutions were made in PBS. For cytoskeletal actin staining, the cell-scaffold constructs were incubated with TRITC-conjugated phalloidin (1:100 dilution) for 60 min. The scaffolds were counter-stained for nuclei with DAPI ((1:300 dilution) for 5 min. After every step, the scaffolds were treated with washing buffer 0.05% of Tween-20 in PBS. Both the TRITC-conjugated phalloidin and DAPI were purchased from CHEMICON International Inc., Temecula, CA. In the end samples were mounted onto a holder with anti-fade mounting solution for immunofluorescence imaging.

2.11. Cell proliferation

Cell proliferation was quantitatively analyzed using a colorimetric assay (MTS, Promega, Madison, WI). At days 3, 7, 14, and 21, cellularized scaffolds were taken out of culture and washed with PBS before moving them into a new well plate containing 1 mL of culture media. Subsequently, 200 μL of 3-(4,5-dimethylthiazol-2-yl)-5-(3-carboxymethoxyphenyl)-2-(4-sulfophenyl)-2H-tetrazolium (MTS) reagent was added to each well and incubated at 37 °C for 2 h. The assay works on the basis that metabolically active cells reduce tetrazolium based MTS reagent to a purplish formazan product. The reaction was stopped by adding 250 μL of 10% sodium dodecyl sulphate (SDS) solution. The resulting solution was diluted in a 4:1 ratio using DDI water (in a new well plate without the scaffold) before recording the absorbance at 490 nm using a Tecan SpectroFluo Plus plate reader (TECAN, Boston, MA). The measured absorbance was compared with the standard curve constructed using known amount of cells and derived the number of cells on a particular scaffold.

2.12. Alkaline phosphatase activity

Alkaline phosphatase activity of cells cultured on microsphere scaffolds was analyzed using an alkaline phosphatase (ALP) substrate kit (Bio-Rad, Hercules, CA). In this assay, the early phenotypic marker ALP, from osteoblasts in culture, converts p-nitrophenyl phosphate (p-

NPP) into p-nitrophenol (p-NP). The rate of p-NP formation is directly proportional to the ALP activity and can be measured colorimetrically. The cell-scaffold constructs were taken out of culture at pre-determined time points (day 7, 14, and 21) and washed twice with PBS to remove any unattached cells. These scaffolds were frozen to −70°C with 1 mL of 1% Triton X100. At the end of the cell study, all the samples were subjected for three freeze-thaw cycles and collected the cell lysate for ALP assay. For a volume of 100 μL of cell lysate, a 400 μL of p-NPP substrate solution and buffer mixture was added and incubated at 37 °C for 30 min. The reaction was stopped by adding 500 μL of 0.4N NaOH. Subsequently, the ALP induced p-NP production was estimated by measuring the absorption at 405 nm. The measured absorbance was normalized by the cell number obtained from the cell proliferation (MTS) assay.

2.13. Statistical Analysis

In vitro studies and the porosity measurements were done in triplicate and n=6 were used for mechanical testing. The quantitative data were reported in the form of mean ± standard deviation. Statistical analysis was performed using a one-way analysis of variance (ANOVA) using Tukey test to determine the statistical significance between the two means evaluated at $p<0.05$.

3. Results

3.1. Polyphosphazenes with higher glass transition temperature for bone tissue engineering applications

Table 1 shows a list of polyphosphazene single-substituent polymers with various amino acid ester groups. We have previously reported glycine and alanine ethyl ester side group polyphosphazenes that showed excellent biocompatibility but lacked the required mechanical strength due to their lower glass transition temperatures.[7–9] In this study we have synthesized three different polyphosphazene single-substituent polymers with amino acid side groups, namely leucine, valine and phenylalanine ethyl esters. Among these, poly[*bis*(ethyl phenylalanato)phosphazene] had a T_g around 41.6 °C which is above the physiological temperature and hence has the potential to be used as scaffold material for load bearing tissue engineering.

3.2. Polyphosphazene- nHAp microspheres

Figure 2 shows SEM micrographs of the PNEPhA microspheres with different nHAp loadings. Pristine PNEPhA microspheres were spherical with smooth surfaces (Figure 2a) while nHAp loaded composite microspheres presented a distorted spherical shape with increased surface roughness. Furthermore, the surface roughness increased with an increase in nHAp content (10 to 30 wt%) as evidenced by Figure 2. Thermo gravimetric analyses confirmed that nHAp content in the composite microspheres was similar to that of the initial loading, and high resolution SEM clearly indicated the presence of nHAp on the surface of the microspheres. The 20% initial loading gave better microsphere yield, and hence that composition was chosen for scaffold fabrication, characterization, and osteoblast performance evaluation.

3.3. Dynamic solvent sintering

Thermal sintering is commonly used to compact microspheres into 3-D structures. The inability to sinter polyphosphazene microspheres by thermal means has led to the development of the solvent/non-solvent sintering method. It was developed based on the concept of fractional solubility defined by Flory-Huggins solution theory, where polymer dissolution and precipitation is well controlled by the polar, dispersive, and hydrogen bonding forces exhibited by the solvents. These fractional parameters are precisely controlled by the solvent/non-solvent composition.[13,14] With respect to these parameters every polymer can have soluble, partially

soluble, and insoluble regions. In the present study THF was selected as a solvent and *n*-hexane as a non-solvent. The final solution composition was chosen in such a way that PNEPhA polymer fell into the partially soluble region to start with and moved towards the insoluble region because of the solvent (THF) evaporation during the course of sintering. Since the solubility parameters of the solution are changing over the sintering time period this method can also be referred to as dynamic solvent sintering. Another criterion for selecting the pair of THF and n-hexane is that the solvent THF is more volatile than the non-solvent n-hexane (at 20 °C THF and *n*-hexane vapor pressures are 129 and 121.2 mm Hg respectively), so the desired transition from the poorly soluble state to insoluble is easily attained during sintering. Also, the solvents are miscible and do not form azeotropes in the desired range of compositions.

Microsphere sintering with a dynamic solvent is represented pictorially in Figure 3. The dynamic solvent wets the microspheres surface, consequently causing the polymer chains to swell and loosen. These chains subsequently interact with adjacent microspheres as long as the solution composition falls in polymer's partially soluble region. The faster evaporation of the solvent compared to the non-solvent drives the solution nature from poor solvent to non-solvent resulting in precipitation of the polymer chains. The chain interactions such as locking, entanglement or intertwining between the two adjacent microspheres become permanent with precipitation and eventually lead to microsphere bonding as shown in Figure 3.

3.4. Effect of solvent and non-solvent composition on the scaffold properties

Figure 4 shows the SEM micrographs of PNEPhA-nHAp composite microsphere scaffolds sintered with various THF/n-hexane compositions. A broad range of dynamic solvent compositions were tried initially to identify a region where the adjacent microspheres can be bonded to form a 3-D porous scaffold. The sinterable region was found to be in the range of 15–22.5 vol% THF composition with n-hexane. Scaffolds sintered with less than 15% did not survive after demolding, while a THF composition higher than 22.5% resulted in polymer dissolution which led to deformed microsphere scaffolds with a decreased degree of porosity. It is readily seen from Figure 4a that scaffolds sintered with 15THF/85hexane exhibited minimal bonding between the microspheres. In contrast 22.5THF/77.5hexane sintered scaffolds showed signs of polymer dissolution (Figure 4d). Necessary bonding between the adjacent microspheres was achieved at compositions between 17.5– 20 THF vol%. Overall, the microsphere fusion, as shown in the high magnification images, was greatly enhanced by increasing THF from 15 to 22.5 vol%.

The solvent sintered scaffolds were characterized for their mechanical strength and the porosity. Scaffolds sintered with THF compositions 17.5, 20 and 22.5 vol% (chosen from the sinterable region) were considered for this study. As shown in Figure 5, these scaffolds showed compressive moduli and the compressive strengths in the range of 45.9±3.7 – 80.5±10 MPa and 6.5±1.6 – 12.9±2.5 MPa respectively. Both the compressive modulus and the compressive strength are increased with increases in THF content. The measured median pore diameter (145.1±4.2 – 86.2±4.6 μm) and the pore volume (23.7±0.8 – 15.1±0.8%) for these scaffolds are shown in Figure 6. The measured pore sizes are in line with the SEM observations. In contrast to the mechanical properties, the pore size and the porosity is found to decrease with an increase in THF content from 17.5 – 22.5 vol%. Based on these properties, 20THF-80hexane solvent sintered scaffolds with optimal mechanical and porosity (compressive modulus and strength 69.5±4.9, 11.2±1.8 & median pore diameter and volume 117.6±6.8 μm, 19.8±0.9%) were chosen for *in vitro* evaluation. From now on, we will refer to the 20THF-80hexane composition as 20T-80H for convenience.

3.5. In-vitro evaluation of Polyphosphazene- nHAp scaffolds

Figure 7 shows the primary rat osteoblast cell proliferation recorded at day 7 on 20T-80H solvent sintered PNEPhA-20HA scaffolds. It is evident from the SEM micrograph that initial cell proliferation is higher at the microsphere junctions. High resolution imaging (shown as inset of Fig 7) revealed well spread cell morphology on the entire microsphere surface. SEM micrographs recorded at later time points (day 14 and 21) showed progressive growth of PRO cells on these scaffolds. This is further corroborated by cytoskeletal actin immunofluorescence staining. Figure 8 shows the cytoskeletal actin distribution recorded on cell-scaffold constructs at day 2, 6 and 12. Actin presence was found to increase with an increase in the culture time. It is found that the initial proliferation is concentrated at bonding regions between microspheres (Figure 8b). Later on cells migrated to microsphere surfaces and became semi-confluent by day 12 as shown in Figure 8c. Because the blue emission of the polymer PNEPhA is interfering with nuclei emission, nuclei fluorescence is not included in the images.

The quantitative cell proliferation data obtained through MTS assay is shown in Figure 9. At day 3 and 7, the number of cells on PNEPhA composite scaffolds was significantly lower than with PLAGA composite scaffolds. However, by day 14 PNEPhA scaffolds showed cell numbers comparable to PLAGA scaffolds. Again, day 21 data showed significantly less cell proliferation on PNEPhA against PLAGA scaffolds. At all time points, tissue culture polystyrene (TCPS) showed significantly higher number of cells than both PNEPhA and PLAGA composite scaffolds. The phenotypic expression of cells cultured on 3-D composite scaffolds was evaluated by monitoring ALP expression levels and shown in Figure 10. At early time points (day 7 and 14) PNEPhA composite scaffolds exhibited lower levels of ALP expression compared to PLAGA. However by day 21, osteoblastic phenotypic expression on PNEPhA composite scaffolds was comparable with the expression on PLAGA and the positive control TCPS.

4. Discussion

Heat sintered PLAGA 85/15, PLAGA-nHAp and PLAGA-chitosan microsphere scaffolds exhibited appropriate mechanical strength, porosity and proved to be potential scaffolds *in vitro* and *in vivo*.[10,11,15,16] The present study aimed to develop polyphosphazene-nHAp composite microsphere scaffolds that closely mimic bone in structure and composition with mechanical properties in the lower range of human cancellous bone.[10] To meet this criterion, we synthesized polymers with bulkier side groups such as leucine, valine and phenylalanine, and these polymers were found to have improved T_g values (Table 1). Of all the polymers studied, the phenylalanine ethyl ester side group polymer PNEPhA showed a T_g (41.6 ± 1 °C), which is one of the highest T_g values reported so far in the class of biodegradable polyphosphazenes. The glass transition temperature is influenced by the steric characteristics of the side groups. Since phenylalanine ethyl ester possesses the large phenyl ring side chain from the amino acid residue, this sterically limits the motion of the polymer backbone. There are also π-π interactions between the phenyl rings that cause the side groups to become ordered. The increase in order also limits the flexibility of the backbone and thus raises the glass transition temperature.

The composite approach has been widely applied to regenerate bone, because native bone tissue is composed of collagen and nano-hydroxyapatite. In order to closely mimic the bone composition, 100 nm sized hydroxyapatite particles were incorporated into PNEPhA microspheres. High resolution SEM indicated the presence of nHAp on the microsphere surface (Figure 11c), which further increased with increases in HAp loading. Because these microspheres are formed in water, and the nHAp is more hydrophilic than PNEPhA, it is expected that more nHAp should be formed on the surface rather than within the bulk of the

microsphere. The presence of nHAp on the scaffold surface is a desired feature that determines the osteogenicity of these scaffolds.[17,18]

A dynamic solvent sintering method was used to develop PNEPhA 3-D scaffolds because the polymer showed thermal decomposition when subjected to heat sintering at temperatures of 80 °C and above. The sintered scaffold macro structure, the bonding between the adjacent microspheres, and the surface nano-topography are shown in Figure 11. The presence of calcium (Ca) and phosphorous (P) in the EDAX spectra (not shown here) confirm the presence of a calcium phosphate phase on/within the microspheres. Since nHAp was added to the polymer PNEPhA and was not subjected to any inorganic acids or heat treatments during the microsphere formation or scaffold fabrication, we assign the P and Ca peaks for the nHAp that is present in the microsphere scaffolds. The high phosphorous (P) content detected here is attributed to the presence of phosphorus in the PNEPhA backbone along with the nHAp. Previous studies have demonstrated higher protein adsorption and increased osteoblast functions on such nanofeatured scaffolds.[17,18] The observed nano-features on the microsphere surface due to nHAp has the potential to positively influence the osteoblast cell adhesion and growth, and to impart enhanced osteointegration to these scaffolds when implanted *in vivo*.

As shown in Figure 3, the dynamic solvent first interacts with the polymer chains on the microsphere surface. This interaction is only feasible when the solubility parameters of the dynamic solvent match the polymer solubility parameters. In addition, the sintering technique requires a combination of solvent and non-solvent, with the solvent being more volatile than the non-solvent. Various trials resulted in THF-hexane combinations that satisfy both these requirements. Solubility parameters of THF, hexane in certain ratios are shown in Table 2.[13, 14] Hexane being 100% dispersive, the addition of hexane to THF results in increased dispersion and decreased polar and hydrogen bonding forces. It is clear from this study that the range of compositions (THF-17.5 to 22.5 vol%, hexane-82.5 to 77.5 vol%) result in PNEPhA-nHAp composite microsphere sintering. Previous study with pure PNEPhA microspheres showed the required dynamic solvent composition as 30 THF + 70 hexane.[12] This can be explained based on the fact that polymer solubility parameters depend on the chain length and the surface morphology when dealing with fractional solubility.[19] In the present case, the lower chain length (Mw is 130 kDa) and the higher surface roughness (a result of nHAp presence on the surface) moved the THF composition to the lower end. Also the polymer dissolution is faster in the present case because of the disruption in the polymer network caused by the presence of nHAp on the microsphere surface.

The bonding between the adjacent microspheres is the key parameter that dictates the microsphere scaffold properties. Although individual microspheres in general show much higher mechanical strength, the 3-D scaffold mechanical properties are often limited by the microsphere-microsphere bond strength. Based on this notion, various dynamic solvent compositions (15 to 22.5 vol% of THF) were utilized and obtained different degrees of bonding between the adjacent microspheres (Figure 4).

Tissue engineering scaffolds should match the native tissue in mechanical properties to support the tissue function, and porosity for cell infiltration, nutrient supply and waste removal. The current effort was to develop polyphosphazene-nHAp microsphere scaffolds that closely match the mechanical and porosity properties of human cancellous bone. PNEPhA-nHAp composite microsphere scaffolds sintered with various dynamic solvent compositions (17.5–22.5 vol% of THF) showed compressive modulus in the range of 46–81 MPa and the compressive strength of 6.5–13 MPa. These values are not only in the lower range of human cancellous bone, but also fall in the range of previously reported scaffold mechanical properties.[10,20,21] Furthermore, the scaffolds showed median pore diameter 145-86 μm and the pore volume 24-15%. The observed pore diameter clearly supports the bone cell migration into these 3-D

scaffolds.[10,22] In an ideal case 30% of the starting porosity would result in 70% of porous tissue that matches the native bone structure. However scaffolds with a pore volume around 20% have illustrated acceptable phenotype progression *in vitro* and defect healing *in vivo* in previous studies.[10,15,16] Based on these previous studies the present scaffolds can be effectively used for *in vivo* bone tissue engineering.

Cytoskeletal actin images recorded at day 2, day 6, and day 12 indicated the increased presence of cytoskeletal actin over the culture period (Figure 8). Microsphere adjoining areas offer high surface area regions per a given volume compared to the non-adjoining regions. High surface area regions attract higher amount of matrix proteins and provide an opportunity for a greater number of cell adhesions per unit volume, leading to increased cell proliferation. Therefore, the adjoining areas (as indicated by a circle in figure 8b) become confluent early compared to the non-adjoining areas. This observation is in line with our previous studies conducted on the PLAGA 85/15, and PLAGA-HAp and PLAGA-chitosan composite microsphere scaffolds.[10,23]

Osteoblast cell adhesion and growth was further corroborated by quantitative cell proliferation recorded using MTS assay. The progressive growth of osteoblasts on PNEPhA composite scaffolds is similar to the trend observed for PLAGA composite scaffolds. The lower levels of ALP expression (at days 7 and 14) on PNEPhA scaffolds suggest the possibility that osteoblasts on these scaffolds may stay in a proliferation phase for a longer period than on PLAGA scaffolds.[24] However, PLAGA equals ALP expression on day 21 indicating the same level of osteoblast maturity on PNEPhA scaffolds. The observed differences in the cell proliferation and the ALP expression between PLAGA and PNEPhA composite scaffolds could be mainly attributed to the difference in the hydrophobicity of these respective materials. PNEPhA being a hydrophobic polymer (compared to PLAGA) allows stronger interactions between the surface and the adhered proteins. This strong interaction would inhibit the adhered cell re-orientation, migration and the cellular phenotypic expression.[25] Work is under progress to further improve the osteogenicity of PNEPhA scaffolds suitable for bone tissue engineering applications.

We have synthesized a number of biodegradable polymers and identified PNEPhA as the one with a glass transition temperature (T_g, 41.6 °C) higher than human body temperature. The current effort has led to 3-D microsphere polyphosphazene-nHAp composite scaffolds with suitable mechanical properties, porosity and osteoblast cell affinity to be used for bone tissue engineering applications. This is a significant achievement because PNEPhA scaffolds with neutral by-products are a potential alternative to acid degrading PLAGA implants or tissue engineered constructs.

5. Conclusions

Biodegradable polyphosphazenes are a unique class of polymers with controllable physicochemical and degradation properties. In this study, we have demonstrated for the first time the feasibility of biodegradable amino acid ester polyphosphazene/nano-hydroxyapatite composite microsphere scaffolds for orthopedic applications. A polymer with a glass transition higher than physiological temperature was synthesized and fabricated into nano-hydroxyapatite-incorporated composite microspheres. Using a novel dynamic solvent method, these microspheres were sintered and optimized to attain suitable porosity and mechanical strength for bone repair/regeneration. Primary rat osteoblast cell adhesion, proliferation and alkaline phosphatase expression on the three dimensional matrices further confirm the potential use of polyphosphazene/nano-hydroxyapatite scaffolds for bone tissue engineering.

Acknowledgement

The authors acknowledge funding from the NIH grant R01 AR052536. Dr. Laurencin is the recipient of the Presidential Faculty Fellow award from the National Science Foundation.

References

1. Allcock, HR. Chemistry and Applications of Polyphosphazenes. Hoboken, NJ: Wiley-Interscience; 2003.
2. Kumbar SG, Bhattacharyya S, Nukavarapu SP, Khan Y, Nair LS, Laurencin CT. J. Inorg. Organomet. Polym 2006;16:365–385.
3. Allcock HR, Pucher SR, Scopelianos AG. Macromolecules 1994;27(5):1071–1075.
4. Ibim S, Ambrosio A, Kwon M, El-Amin S, Allcock H, Laurencin CT. Biomaterials 1997;18:1565–1569. [PubMed: 9430340]
5. Swaminathan, S. Ph.D dissertation. 2005. Low Temperature Setting Polymer-Ceramic Composites for Bone Tissue Engineering. Submitted to Drexel University
6. Laurencin CT, Koh HJ, Neenan TX, Allcock HR, Langer R. J. Biomed. Mater. Res 1987;21:1231–1246. [PubMed: 3693386]
7. Nair LS, Lee DA, Bender JD, Barrett EW, Greish YE, Brown PW, Allcock HR, Laurencin CT. J. Biomed. Mater. Res. A 2006;76:206–213. [PubMed: 16265637]
8. Deng M, Nair LS, Nukavarapu SP, Kumbar SG, Jiang T, Krogman NR, Singh A, Allcock HR, Laurencin CT. Biomaterials 2008;29:337–349. [PubMed: 17942150]
9. Sethuraman S, Nair LS, El-Amin S, Farrar R, Nguyen MT, Singh A, Allcock HR, Greish YE, Brown PW, Laurencin CT. J. Biomed. Mater. Res 2006;77:679–687.
10. Borden M, El-Amin SF, Attawia M, Laurencin CT. Biomaterials 2003;24:597–609. [PubMed: 12437954]
11. Jiang T, Abdel-Fattah WI, Laurencin CT. Biomaterials 2006;27:4894–4903. [PubMed: 16762408]
12. Brown JL, Nair LS, Laurencin CT. J. Biomed. Mater. Res. B. (in press).
13. Phenix A. Kunsttechnologie und Konservierung 1998;12:397–409.
14. http://palimpsest.stanford.edu/packages/solvent_solver.html
15. Khan Y, El-Amin SF, Laurencin CT. Conf. Proc. IEEE. Eng. Med. Biol. Soc 2006;1:529–530. [PubMed: 17946840]
16. Borden M, Attawia M, Khan Y, El-Amin SF, Laurencin CT. J. Bone. Joint. Surg 2004;86:1200–1208.
17. Sato M, Aslani A, Sambito MA, Kalkhoran NM, Slamovich EB, Webster TJ. J. Biomed. Mater. Res. A 2008;84:265–272. [PubMed: 17607739]
18. Nukavarapu, SP.; Kumbar, SG.; Nair, LS.; Laurencin, CT. Biomedical Nanostructures. John Wiley & Sons, Inc.; 2007. Chapter 15; p. 371-401.
19. Hansen, CM. Hansen Solubility Parameters. New York: CRC press; 2000.
20. Ishaug-Riley SL, Crane-Kruger GM, Yaszemski MJ, Mikos AG. Biomaterials 1998;19:1405–1412. [PubMed: 9758040]
21. Wei G, Ma PX. Biomaterials 2004;25:4749–4757. [PubMed: 15120521]
22. Yang S, Leong KF, Du Z, Chua CK. Tissue. Eng 2001;7:679–689. [PubMed: 11749726]
23. Jabbarzadeh E, Jiang T, Deng M, Nair LS, Khan YM, Laurencin CT. Biotechnol. Bioeng 2007;98:1094–1102. [PubMed: 17497742]
24. Wilson CJ, Clegg RE, Leavesley DI, Pearcy MJ. Tissue. Eng 2005;11:1–18. [PubMed: 15738657]
25. Conconi MT, Lora S, Menti AM, Carampin P, Parnigotto PP. Tissue. Eng 2006;12:811–819. [PubMed: 16674294]
26. Singh A, Krogman NR, Sethuraman S, Nair LS, Sturgeon JL, Brown PW, Laurencin CT, Allcock HR. Biomacromolecules 2006;7:914–918. [PubMed: 16529431]

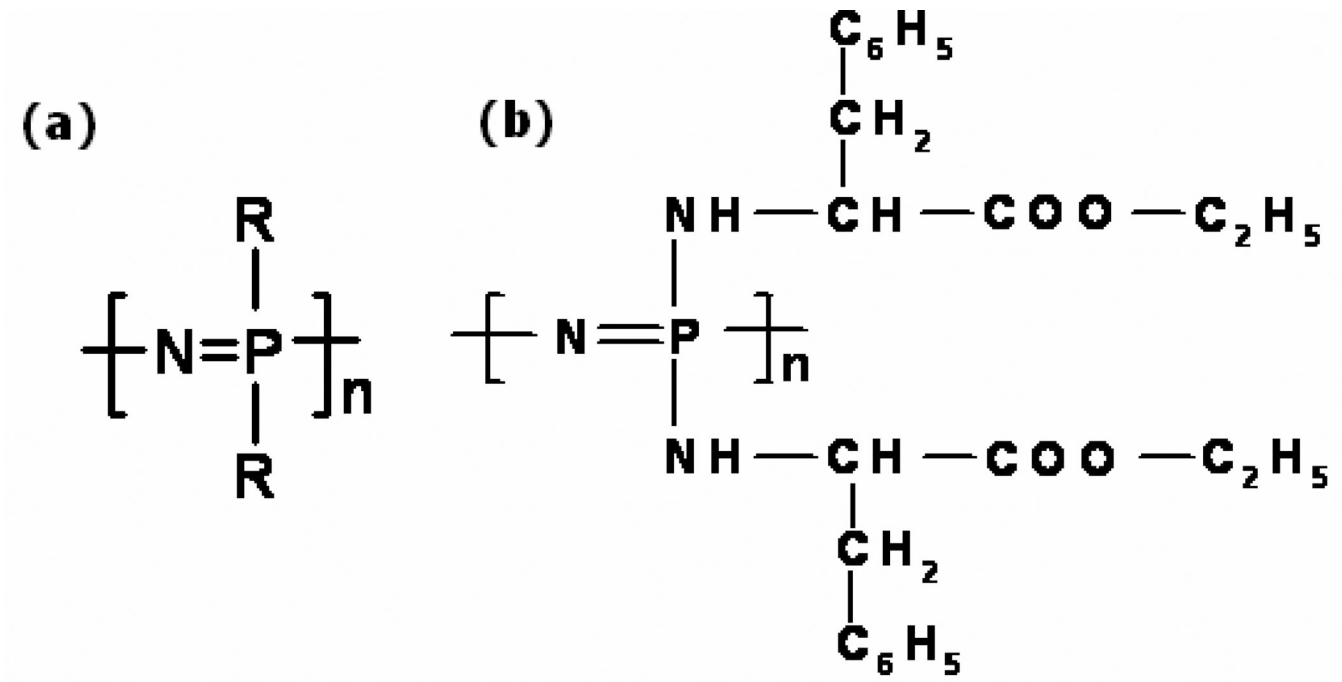

Figure 1.
Structure of (a) general polyphosphazene (PPH) and (b) poly[*bis*(ethyl phenylalaninato) phosphazene] (PNEPhA). PNEPhA is a biodegradable polymer with a glass transition temperature close to popular polyester PLAGA 85/15.

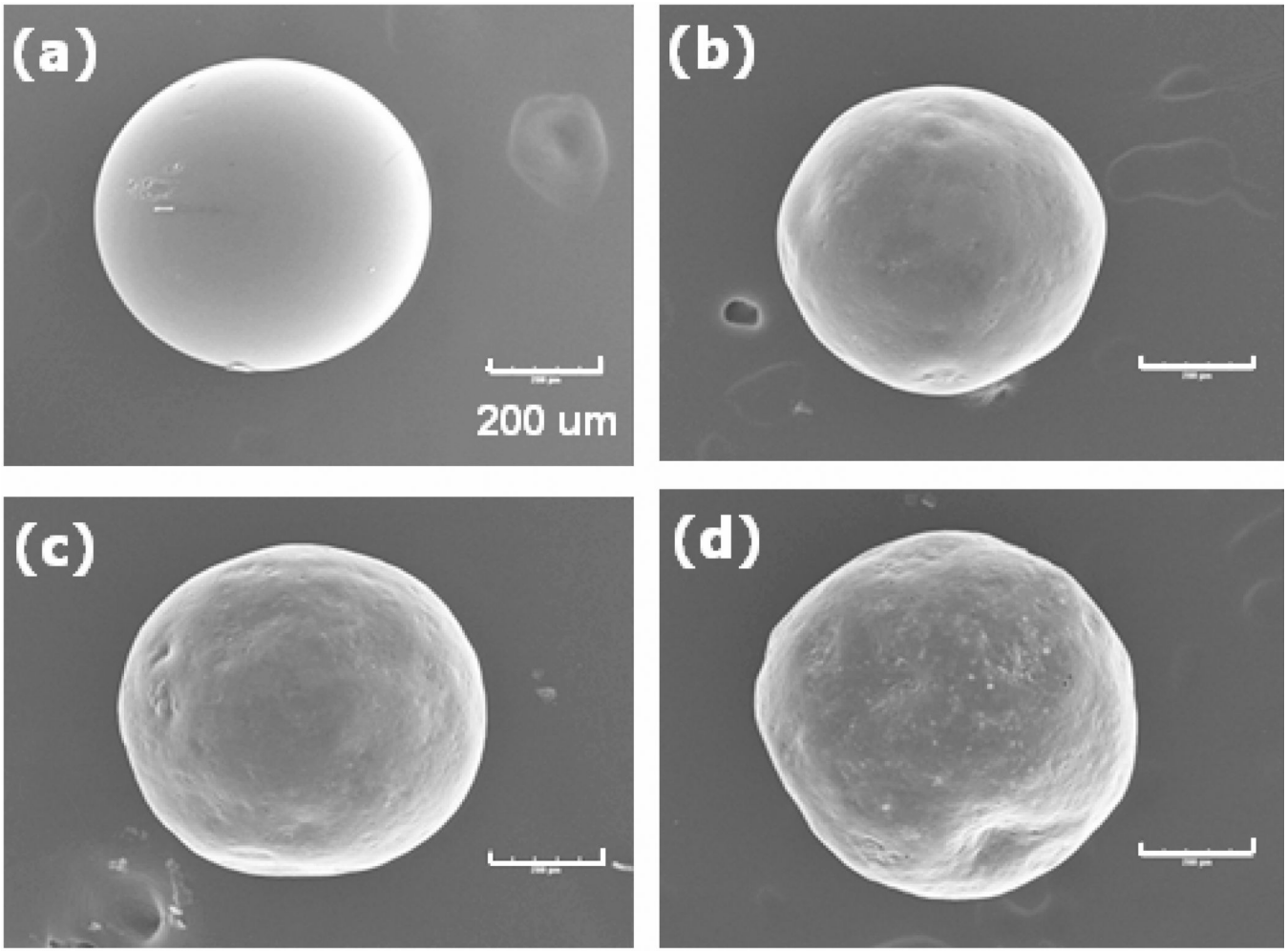

Figure 2.
Scanning electron micrographs of polymer (a) PNEPhA, and composite (b) 90PNEPhA-10nHAp, (c) 80PNEPhA-20nHAp and (d) 70PNEPhA-30nHAp microspheres. The presence of nHAp on the microsphere surface resulted in surface roughness, and the roughness increased with nHAp loading. However, composite microspheres did not form beyond 30% of nHAp loading

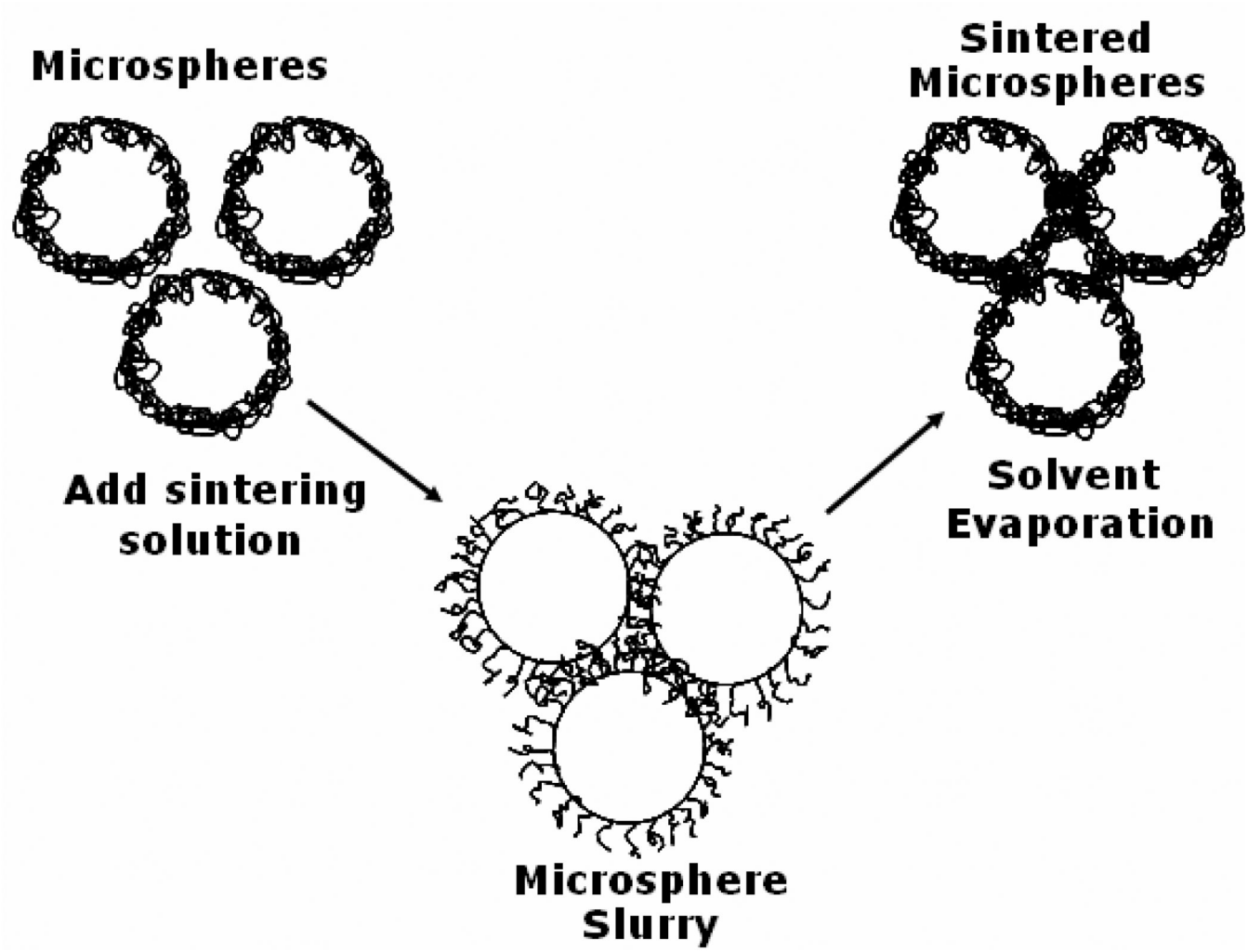

Figure 3.
Schematics of composite microsphere sintering: a solvent/non-solvent approach. In the presence of a dynamic solvent, microsphere surfaces swell and open up the polymer chains. The chain interaction between the adjacent microspheres leads to microsphere bonding. With continued solution evaporation (solvent more than non-solvent), the dynamic solvent transforms from a poor solvent to a non-solvent state, resulting permanent bonding between the adjacent microspheres.

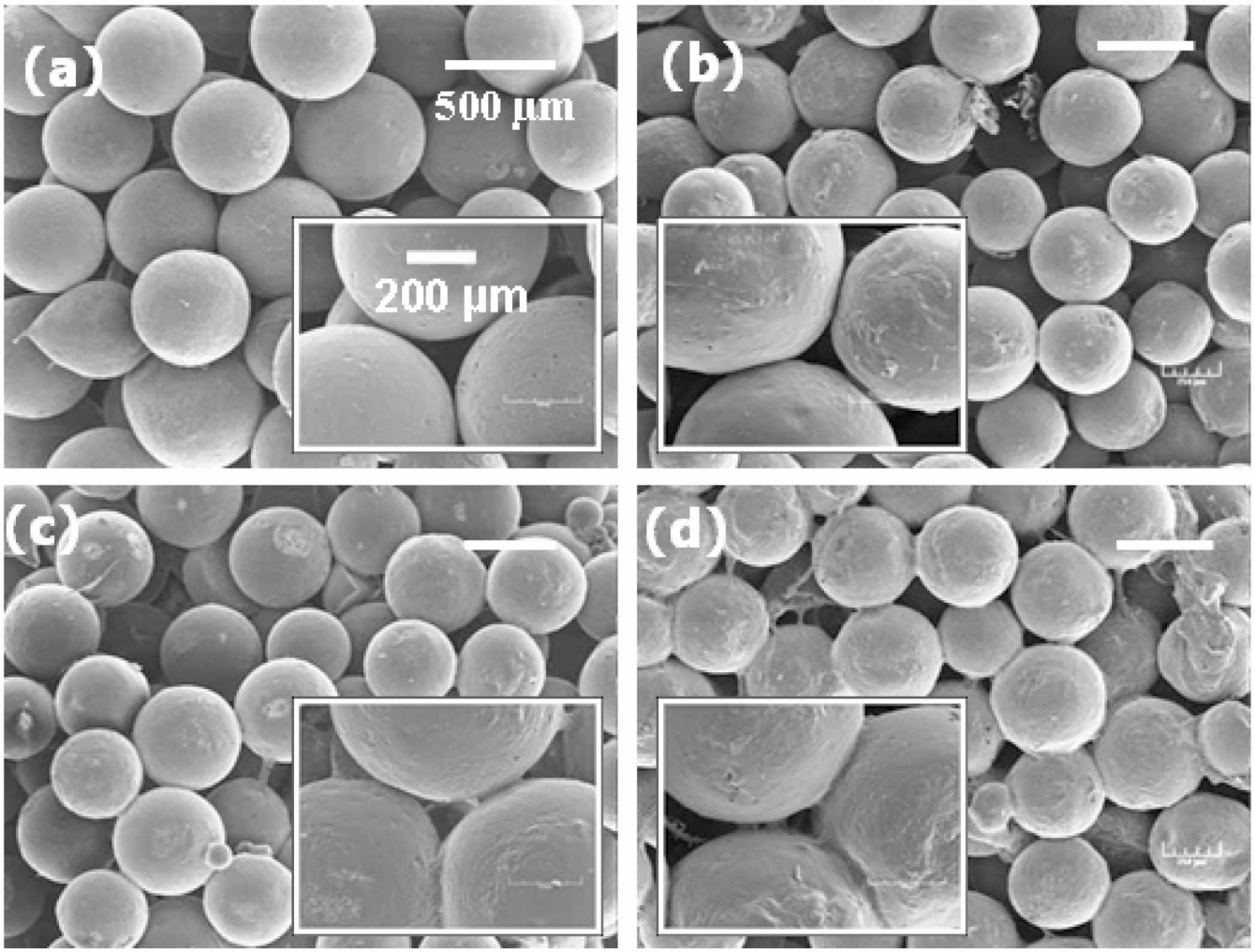

Figure 4.
Scanning electron micrographs showing the morphology of the scaffolds sintered using solvent/non-solvent compositions of (a) 15T-85H, (b) 17.5T-87.5H, (c) 20T-80H and (d) 22.5T-77.5H. Three-dimensional scaffolds showed an interconnected pore structure and the inset shown for every scaffold confirms the bonding between the adjacent microspheres. Where T is for THF and H is for hexane.

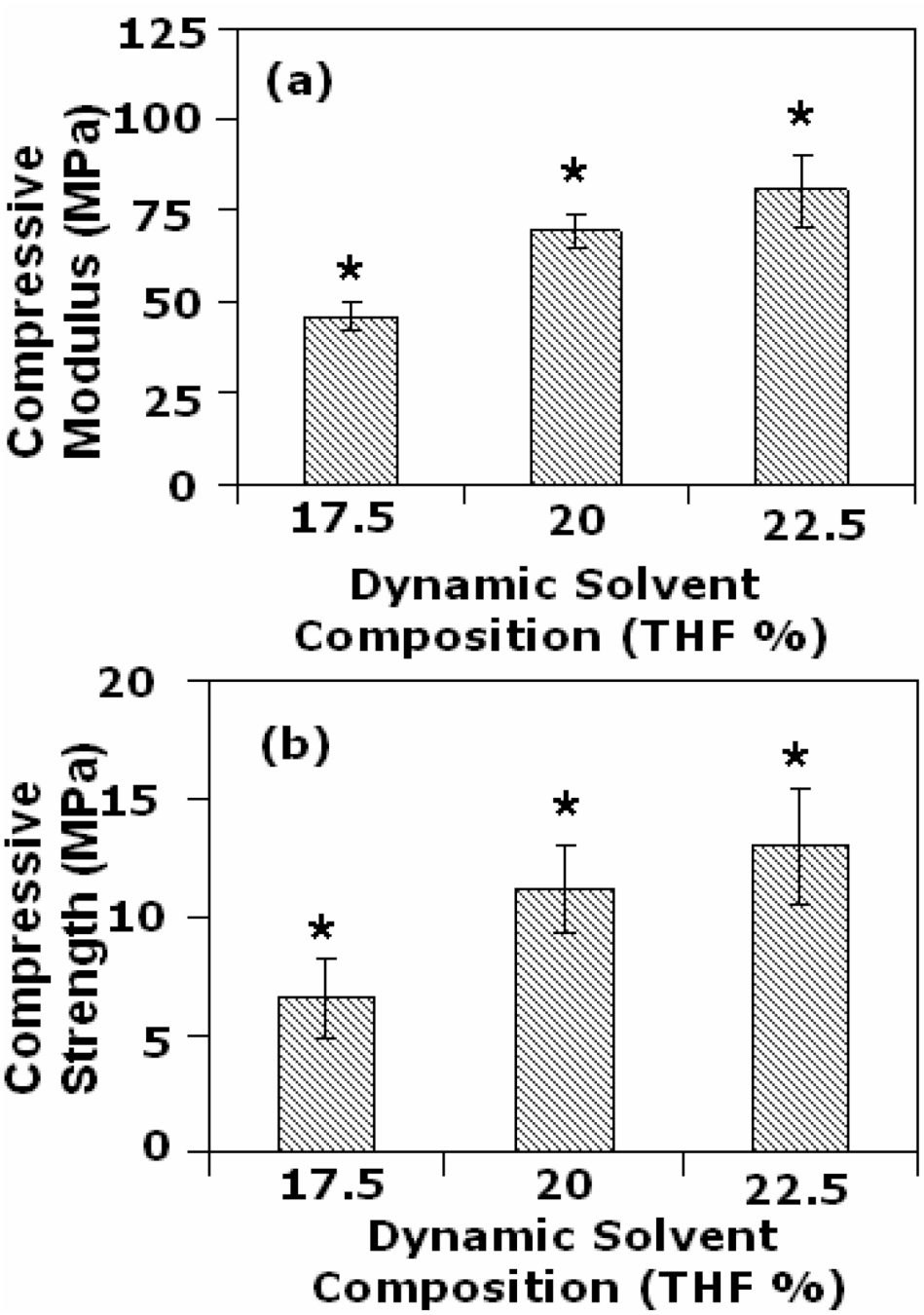

Figure 5.
Effect of solvent/non-solvent composition on scaffold mechanical properties, where (a) is compressive modulus, and (b) is compressive strength. Both compressive modulus and the compressive strength increase with increase with THF content in the dynamic solvent. (*) Denotes significant difference with $p<0.05$.

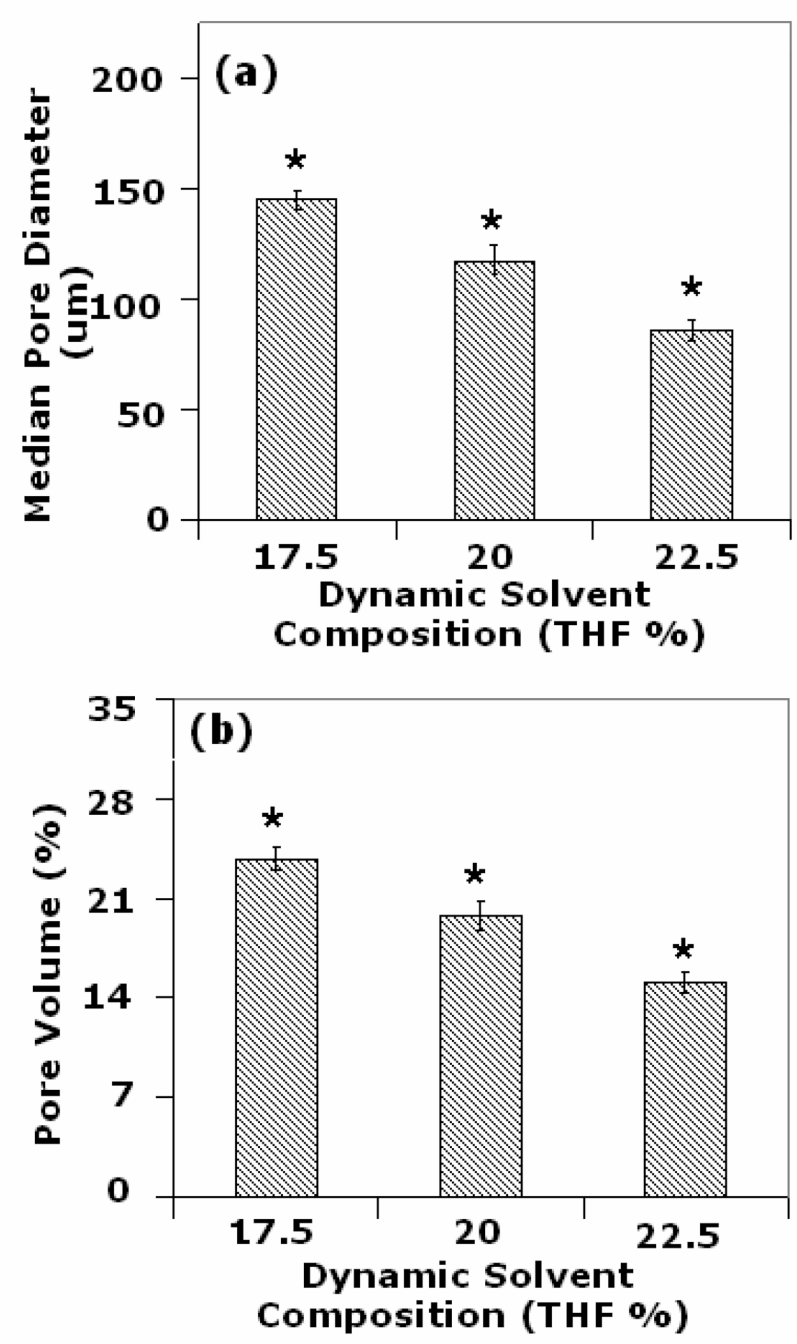

Figure 6.

Effect of solvent/non-solvent composition on scaffold porosity properties, where (a) is median pore diameter, and (b) is pore volume (%). Both pore size and percent of porosity, evaluated using mercury porosimetry, show a decreasing trend with increasing THF content in the dynamic solvent. (*) denotes significant difference with $p<0.05$.

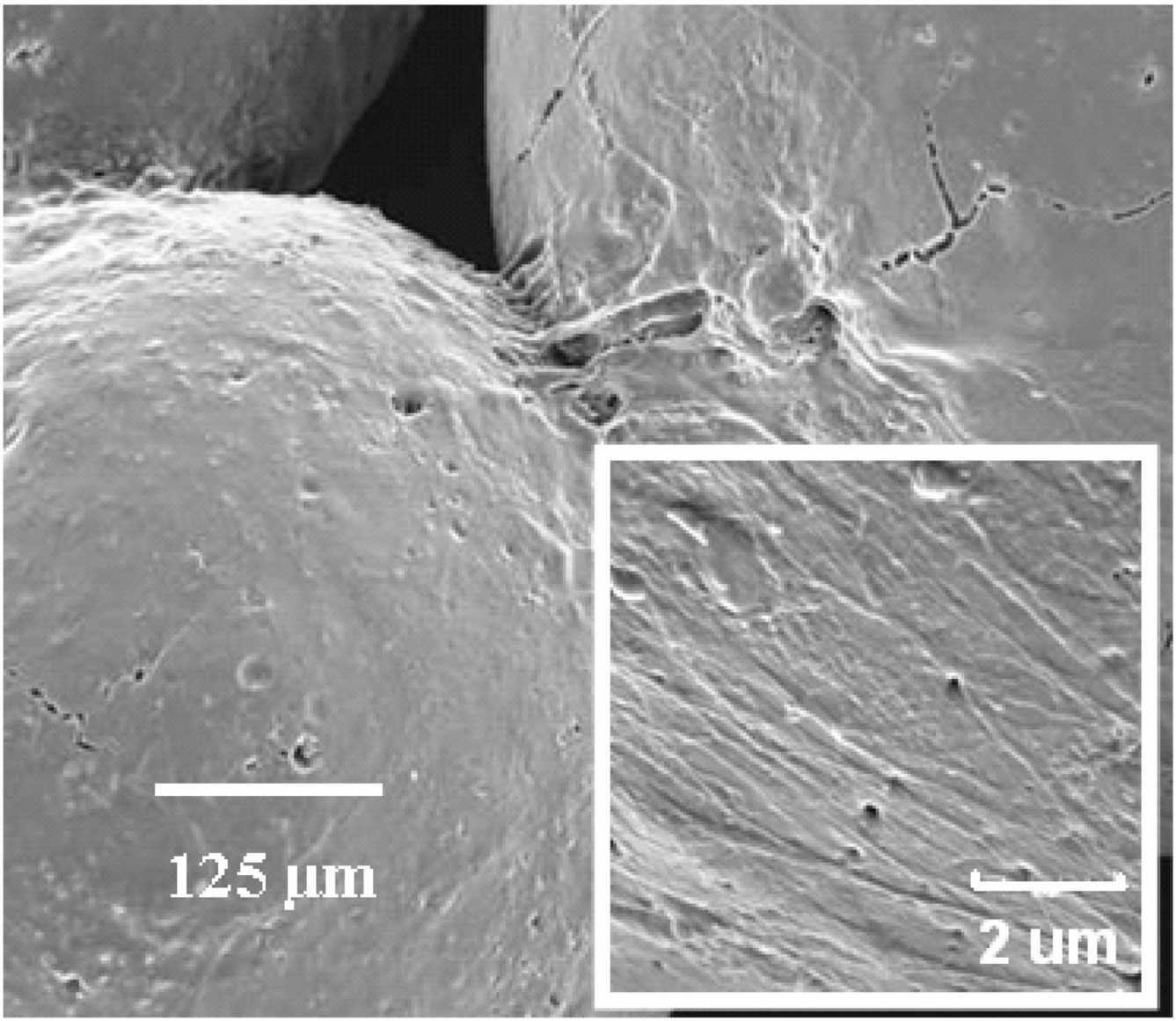

Figure 7.
Scanning electron micrograph showing primary rat osteoblast cell proliferation recorded at day 7. Cell presence is clearly seen in the microsphere adjoining areas. Well spread cells on the microsphere surface (other than the microsphere junctions) are shown in the inset.

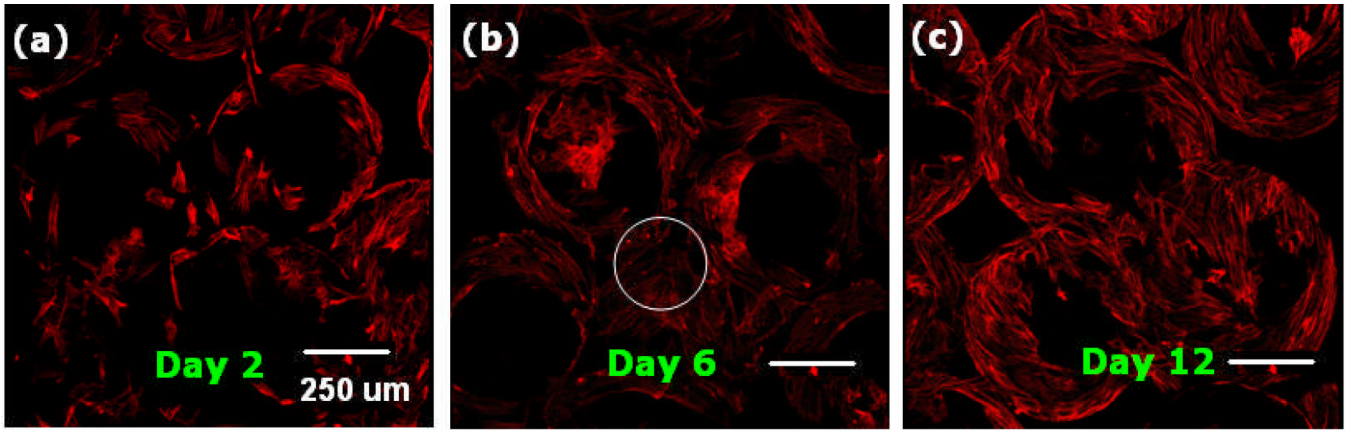

Figure 8.
Cytoskeletal actin distribution of primary rat osteoblast cells grown on composite microsphere matrix for (a) 2, (b) 6 and (c) 12 days. The circled region shows higher initial cell proliferation at the microsphere adjoining areas. DAPI (nuclei stain) emission is not included because of its interference with polymer PNEPhA blue emission.

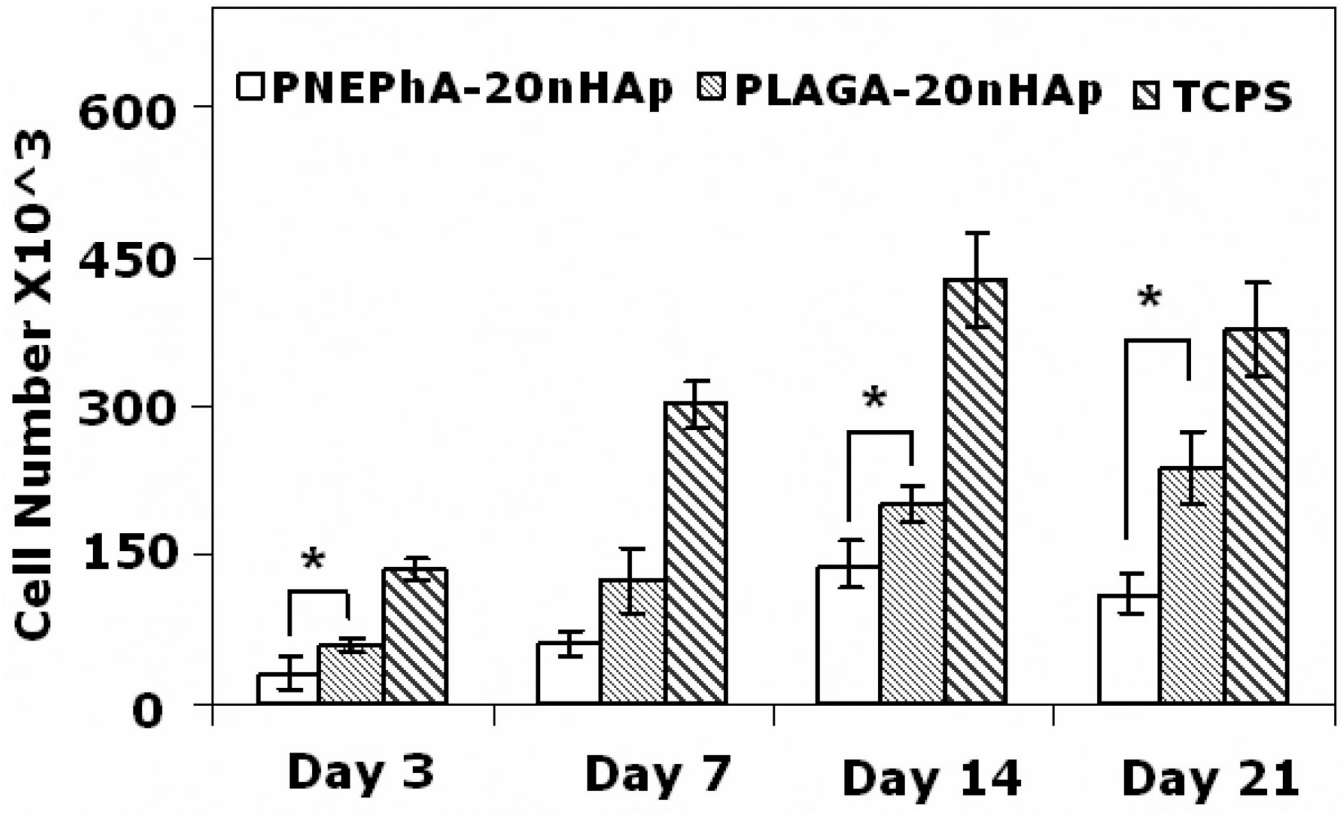

Figure 9.
Primary rat osteoblast cell proliferation (MTS assay) on PNEPhA-20nHAp, PLAGA-20nHAp composite scaffolds and planar TCPS. Progressive growth on TCPS surface is a sign of a healthy PRO culture. (*) Denotes significant difference with $p<0.05$.

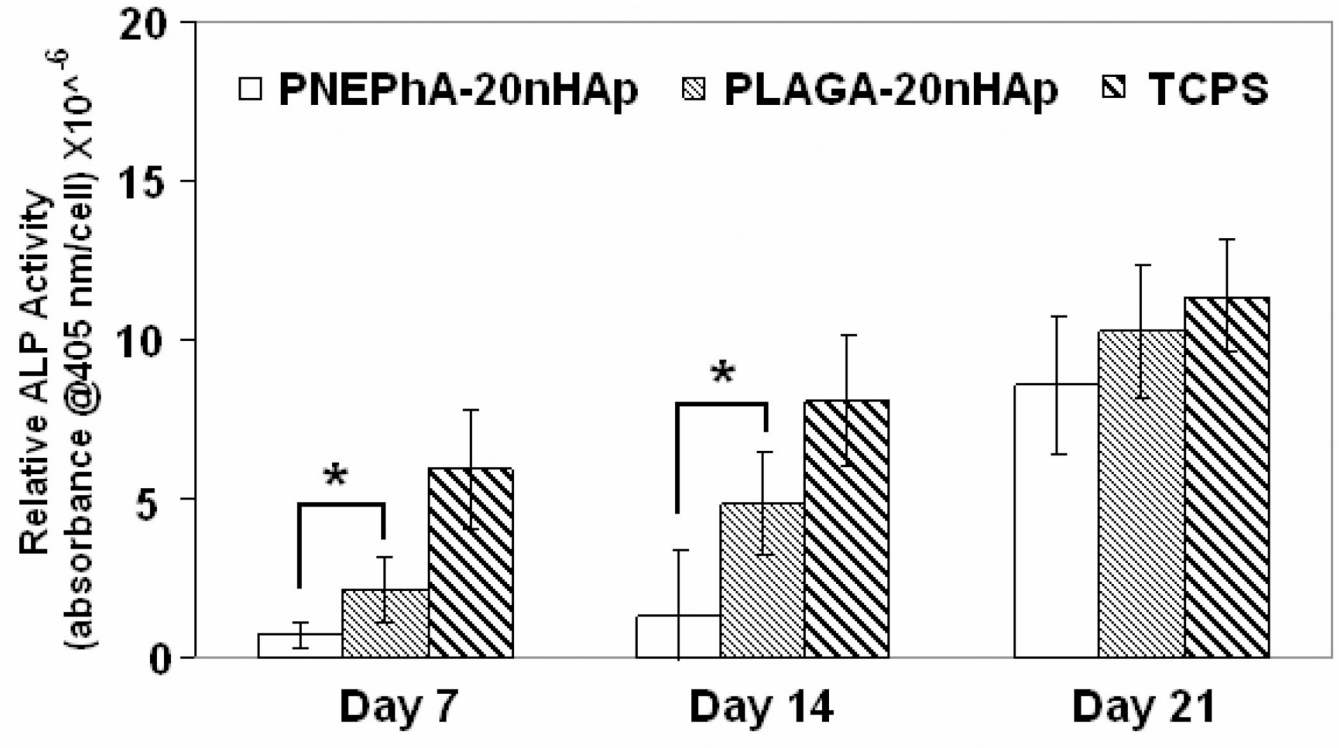

Figure 10.
Alkaline phosphatase activity expressed by primary rat osteoblast cells on PNEPhA-20nHAp, PLAGA-20nHAp composite scaffolds and planar TCPS. (*) Denotes significant difference with $p<0.05$.

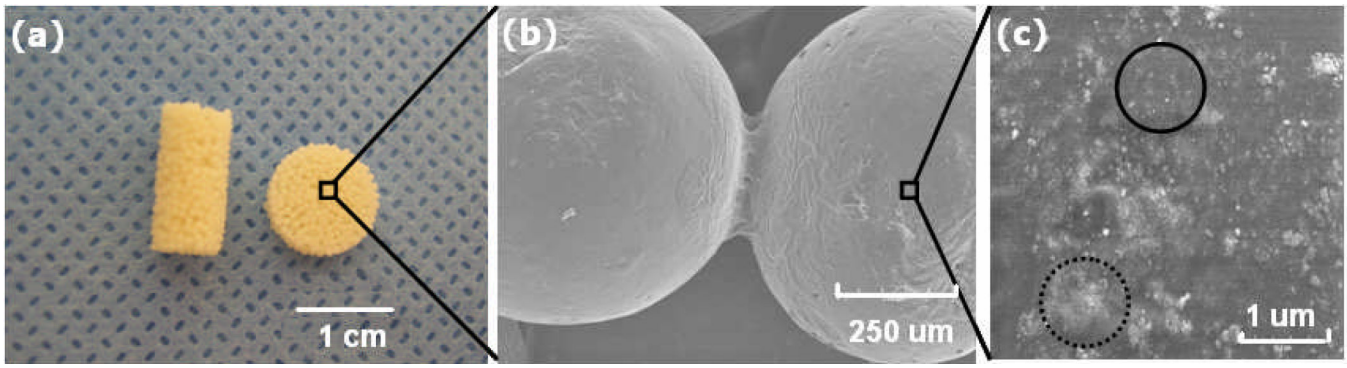

Figure 11.

Macro, micro and nano structure of PNEPhA-20 nHAp composite microsphere scaffolds. (a) Optical image showing cylindrical (10 mm length & 4.5 mm diameter) and disk (2 mm thick & 8 mm diameter) shaped scaffolds fabricated using the dynamic solvent sintering method. Cylindrical scaffolds were used for mechanical testing, and disk shaped scaffolds for porosity and *in vitro* cell studies. (b) SEM showing the microstructure of the scaffolds where the adjacent microspheres are fused via the dynamic solvent sintering method. (c) High magnification scanning electron micrograph showing nano HAp particle dispersion on a microsphere surface. The circled regions show nHAp mono (solid line) and poly (dotted line) dispersion.

Table 1

List of polyphosphazene single-substituent polymers and their glass transition temperatures

R (amino acid ester group)	Corresponding Aminoacid	Tr Ten (
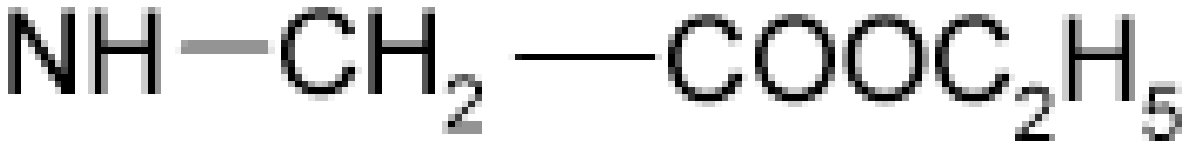	Glycine (gly)	-
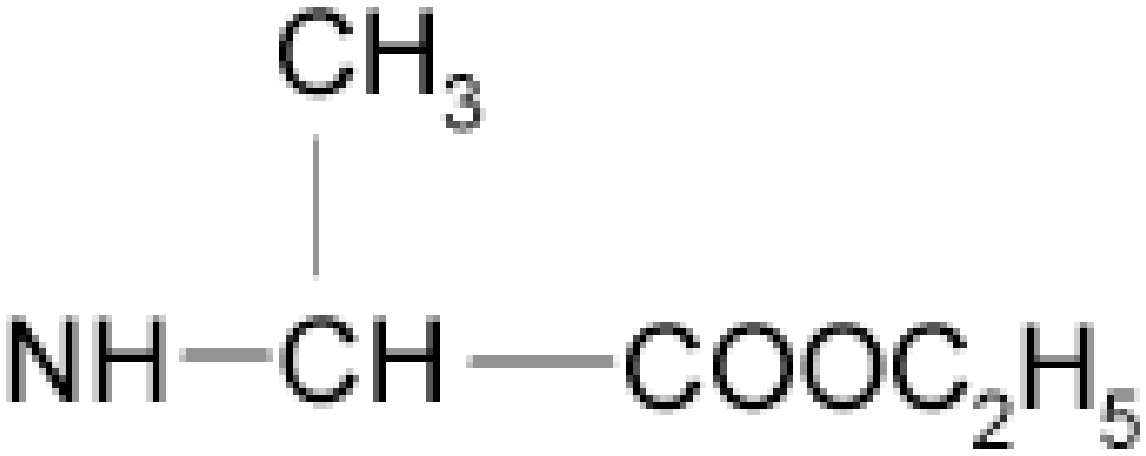	Alanine (ala)	-
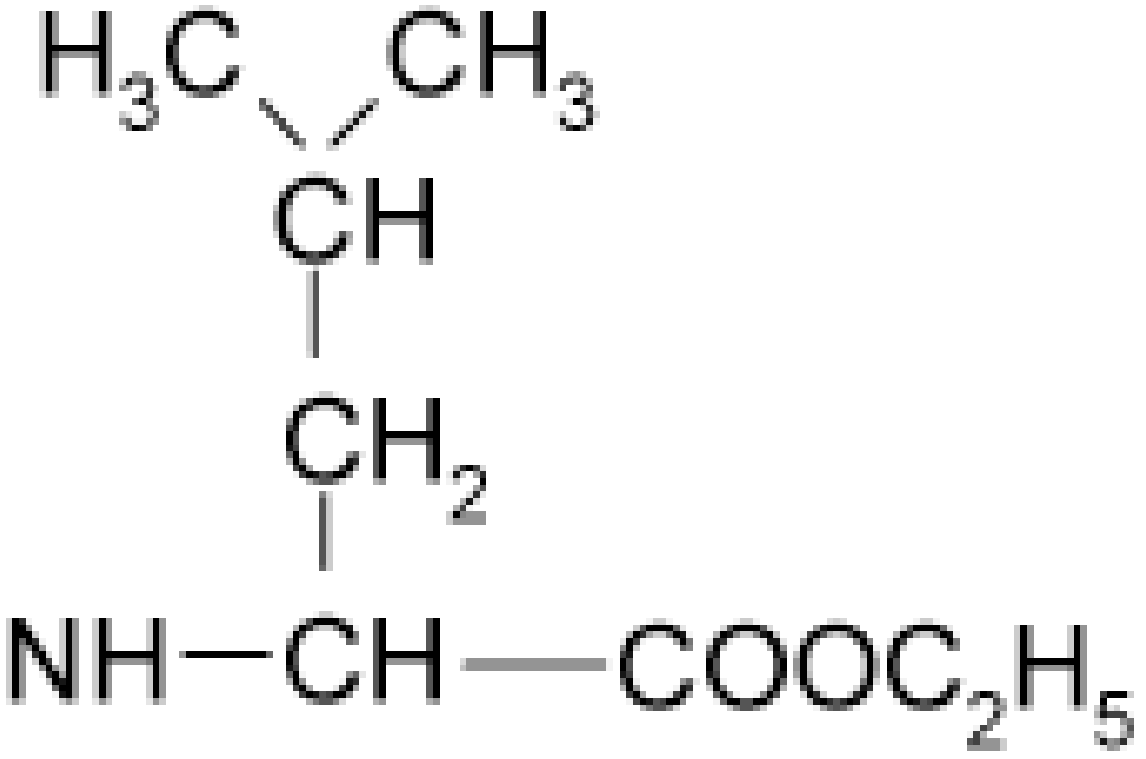	Leucine (leu)	1

R (amino acid ester group)	Corresponding Aminoacid	Tr Ten (
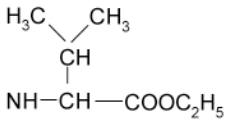	Valine (val)	2
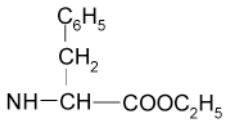	Phenylalanine (phe)	4

Table 2

Dynamic solvent fractional parameters used for mesosphere sintering. Fractional solubility parameters for THF and hexane were obtained from the literature.[13,14] These parameters along with the respective molar volume fractions were further used to calculate the fractional solubility parameters for the dynamic solvents used for sintering.

Solvent/Dynamic solvent	Solvent fractional parameters		
	Dispersion (D)	Polar (P)	Hydrogen bonding (H)
THF (T)	55	19	26
Hexane (H)	100	0	0
17.5T-22.5H	88.78	4.73	6.47
20T-80H	87.35	5.34	7.31
22.5T-77.5H	84.75	6.53	8.93